ACS OMEGA

http://pubs.acs.org/journal/acsodf

Article

3D Numerical Study of the Electrokinetic Motion of a Microparticle Adsorbed at a Horizontal Oil/Water Interface in an Infinite Domain

Chengfa Wang* and Qi Gao

Cite This: *ACS Omega* 2022, 7, 4062−4070

Read Online

ACCESS | Metrics & More | Article Recommendations | Supporting Information

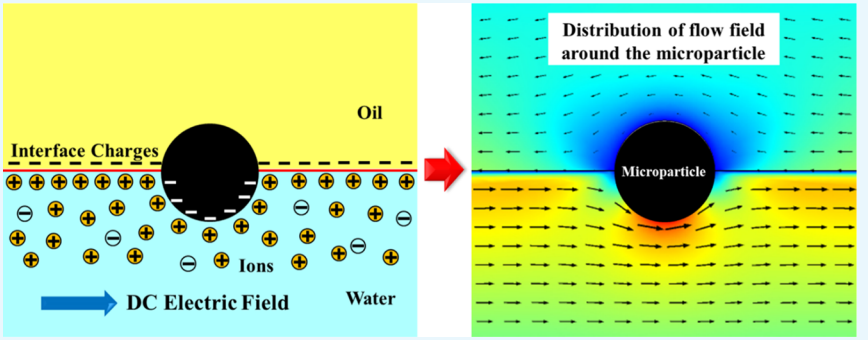

ABSTRACT: This work builds a three-dimensional (3D) simulation model and studies the electrokinetic velocity of a microparticle adsorbed at a horizontal oil/water interface in an infinite domain. The effects of the interface zeta potentials, the electric field, the oil dynamic viscosity, and the contact angle between the particle and the oil/water interface are investigated in detail. The results show that in an infinite oil/water interface system, both the negatively charged mobile oil/water interface and the negatively charged particle adsorbed to it move toward the positive electrode of the DC electric field, and the particle velocity increases along with the contact angle, the electric field strength, and the absolute values of negative zeta potential of both the particle and the oil/water interface. When the oil/water interface is positively charged with a relatively small zeta potential, the negatively charged microparticle also moves in the opposite direction of the electric field. The larger the oil dynamic viscosity, the smaller the electrokinetic velocity of the microparticle at the interface. Additionally, the numerical simulation results are compared with the reported experiment results under the same conditions, and they have good agreement.

1. INTRODUCTION

Electrokinetic phenomena are widely used for manipulating cells and micro-and-nano-particles for biological or chemical analysis.[1−3] For a charged microparticle absorbed at a horizontal oil/water interface in an infinite domain, after a DC electric field is applied to the water domain in a direction tangent to the interface, owing to the electrokinetic phenomena produced at the interfaces with charge, the mobile oil/water interface and the particle at the interface will move, which can be used to sort and manipulate microparticles at a liquid−fluid interface. Many potential and valuable applications, such as water purification and sewage disposal, could be developed from the above phenomena.

Generally, the surface charges could attract the counterions in an aqueous solution and engender the electric double layer (EDL) near the surface. Then, the electrokinetic phenomenon will be generated in the EDL by an applied electric field.[4] Research shows that the liquid−fluid interfaces are usually charged,[5−11] so the EDL can form near an oil/water interface. When a DC electric field is applied to the water phase in a direction tangent to the oil/water interface, the electroosmotic flow (EOF) will form near, and the interface charges will suffer a force derived from the DC electrical field, causing the movement of the interface. Gao et al.[12] developed a model and conducted a detailed study on the electrokinetic phenomenon generated at a charged liquid−fluid interface in a rectangular microchannel. Subsequently, Lee et al.[13,14] experimentally verified Gao's model for the two-liquid electrokinetic phenomenon. Other two-phase electrokinetic phenomenon studies can be found in refs 15−18.

Owing to the electrokinetic phenomenon formed at the oil/water interface, a charged microparticle at the interface will be affected by an electric force from the DC electric field, and two hydrodynamic forces produced simultaneously by the water and oil, thereby making the particle move at the interface. Till date, many published papers report the spontaneous behavior

Received: September 29, 2021
Accepted: January 14, 2022
Published: January 26, 2022

https://doi.org/10.1021/acsomega.1c05405
ACS Omega 2022, 7, 4062−4070

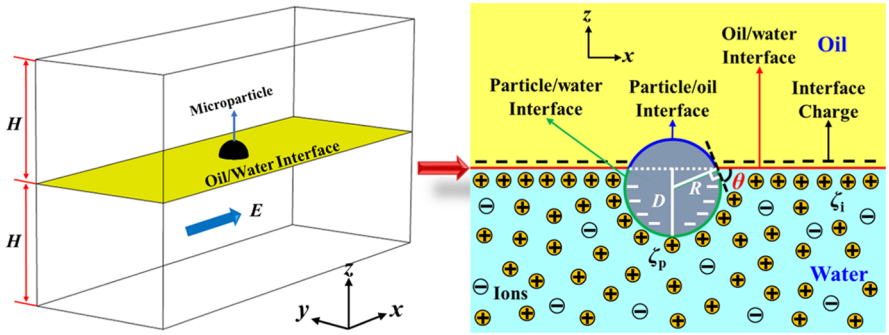

Figure 1. Schematic diagram of the oil/water interface system.

of particles at one interface in the absence of the electric field,[19−27] and, however, very few studies present the electrokinetic behavior of a single microparticle adsorbed at one interface. Boneva et al.[28] experimentally observed the motion of an individual glass particle adsorbed at the water/tetradecane interface under an electric field applied to the tetradecane phase. In the water phase, there is no EOF because of the inexistence of the electric field. Therefore, the motion mechanism of the interfacial particle in their study is different from that in this work. Li and Li[29,30] experimentally found that positively charged nanoparticles absorbed at an oil droplet surface move toward the negative electrode of the DC electric field and congregate on one side of the droplet but did not discuss the effect of the interface electrokinetic phenomenon on the particle motion in detail.

If the oil/water system is in a microchannel, the motion of the interface will be influenced by the EOF formed on the channel wall. In contrast, if the system is infinite, the distance between the wall EOF and the oil/water interface is so far that they do not interact with each other. Therefore, the electrokinetic behavior of a microparticle adsorbed at one horizontal interface in an infinite domain is quite different from that in a microchannel. We have previously carried out a detailed theoretical study on the electrokinetic velocity of a single microparticle at a horizontal oil/water interface in a microchannel and found the negatively charged oil/water interface and microparticle usually all move toward the negative electrode of the DC electric field applied to the water.[31] Zhang et al.[32] carried out an experimental investigation on the electrokinetic behavior of a polystyrene particle at the dodecane/water interface with an infinite domain and found the particle at the interface moves toward the positive electrode of the DC electric field. However, some parameters, such as the interface zeta potentials and the contact angle between the particle and the interface, are hard to adjust due to the limitation of the experimental conditions and still need further study and theoretical analysis.

This work develops a theoretical model and numerically investigates the electrokinetic velocity of a microparticle at the horizontal oil/water interface in an infinite domain for the first time. The influence factors, such as the contact angle between the particle and the oil/water interface and the interface zeta potentials, are emphatically studied and analyzed. Furthermore, to verify the model established in the paper, the numerical simulation results are also compared with Zhang's experiment results.

2. OIL/WATER INTERFACE SYSTEM AND A THEORETICAL MODEL

Figure 1 displays the infinite oil/water interface system studied in this work. The center of the horizontal oil/water interface is set to be the coordinate origin. The heights of the oil domain and the water domain are the same and denoted by H. A spherical microparticle with radius R = 5 μm is adsorbed at the oil/water interface, and θ stands for the contact angle between the particle and the interface (see Figure 1). The contact angle (θ) determines the location of the microparticle at the oil/water interface. $\theta < 90°$ means the particle is relatively hydrophilic, and a hydrophobic particle usually has a larger value ($\theta > 90°$). In other words, the smaller the contact angle, the larger the immersion depth (D) of the particle in the water. ζ_p is the particle zeta potential, and ζ_i denotes the zeta potential of the oil/water interface. The larger the zeta potential value, the greater the surface charge density. Additionally, if the zeta potential value is negative, the surface is negatively charged. As shown in Figure 1,[33,34] EDLs will be generated near the interfaces due to the interaction between interface charges and ions distributed in the water. After the DC electric field ($\boldsymbol{E}$) is applied to the water along the x-axis, the electrokinetic phenomenon will form near the oil/water interface, driving the interface and the corresponding particle to move. Thus, the theoretical model is as follows.

The distribution of the DC electric potential (V) field is described using the Laplace equation

$$\nabla^2 V = 0 \tag{1}$$

The relationship between the electric potential and the electric field strength ($\boldsymbol{E}$) is as follows

$$\boldsymbol{E} = -\nabla V \tag{2}$$

In the water domain, the right boundary is grounded, and a voltage that determines the electric field strength is applied on the left.

Owing to the surface charges and the accumulated counterions, the net charge density is not zero in EDLs. The Poisson−Boltzmann (PB) equation[35] governs the distribution of the electric potential (ζ) in EDLs

$$\nabla^2 \zeta = -\frac{\rho_e}{\varepsilon_0 \varepsilon} \tag{3}$$

where $\varepsilon_0 = 8.85 \times 10^{-12}$ F/m is the vacuum permittivity, ε = 80 is the relative permittivity of the water, and ρ_e is the local net charge density, given by

https://doi.org/10.1021/acsomega.1c05405
ACS Omega 2022, 7, 4062−4070

$$\rho_e = -2zen_\infty \sinh\left(\frac{ze\zeta}{k_B T}\right) \tag{4}$$

where ζ denotes the local electric potential in the EDL; $z = 1$ (this model assumes the electrolyte in the water phase is KCl) and $e = 1.602 \times 10^{-19}$ C are the absolute value of ionic valence and the elementary charge, respectively; $n_\infty = C_0 N_A$ ($N_A = 6.022 \times 10^{23}$ mol^{-1} is the Avogadro constant, and $C_0 = 0.001$ mol/m^3 is the ionic concentration.) stands for the ionic number concentration in the water phase; $k_B = 1.38 \times 10^{-23}$ J/K is the Boltzmann constant; and $T = 298$ K is the absolute temperature. The corresponding boundary conditions are as follows

$$\zeta = \zeta_i \tag{5}$$

at the oil/water interface marked with red color

$$\zeta = \zeta_p \tag{6}$$

at the particle/water interface marked with green color.

The flow field is determined by the well-known Navier–Stokes (NS) equation and the continuity equation. Their steady-state expressions are as follows

$$\rho \boldsymbol{U}\cdot\nabla \boldsymbol{U} = -\nabla p + \mu\nabla^2 \boldsymbol{U} + \boldsymbol{F} \tag{7}$$

$$\nabla\cdot\boldsymbol{U} = 0 \tag{8}$$

where ρ and μ denote the density and the dynamic viscosity of the liquid, respectively; p is the pressure, $\boldsymbol{F}$ is the body force, and $\boldsymbol{U}$ is the velocity vector.

As the DC electric field applies an electric force to the net charges in the EDLs, the NS equation in the water phase is given by

$$\rho_w \boldsymbol{U}_w\cdot\nabla \boldsymbol{U}_w = -\nabla p + \mu_w\nabla^2 \boldsymbol{U}_w + \rho_e \boldsymbol{E} \tag{9}$$

where $\rho_w = 1000$ kg/m^3 and $\mu_w = 0.001$ Pa·s are the density and the dynamic viscosity of the water, respectively, and $\boldsymbol{U}_w$ is the velocity vector of the water.

Since the DC electric field is only applied to water, and the EDL cannot form in the oil, the oil does not suffer the electric force. Therefore, for the oil, the NS equation is simplified to

$$\rho_o \boldsymbol{U}_o\cdot\nabla \boldsymbol{U}_o = -\nabla p + \mu_o\nabla^2 \boldsymbol{U}_o \tag{10}$$

where $\rho_o = 900$ kg/m^3 and $\mu_o = 0.001$ Pa·s are the density and the dynamic viscosity of the oil, respectively, and $\boldsymbol{U}_o$ is the velocity vector of the oil.

In this model, the water and oil flow are dependent on the electrokinetic phenomenon, and all boundaries are free from external pressure. Thus, there should be zero pressure boundary conditions on the inlet and outlet boundaries of the oil and water domains.

Since the energy of the EOF is low, the effect of the EOF becomes weak when the distance from the surface is large enough. In this work, the domain of the oil/water interface system is infinite, namely that the distance between the interface and the bottom boundary is large enough, which means the EOF generated on the bottom does not affect the mobile oil/water interface. Thus, the simplified no-slip boundary condition was applied at the top and bottom boundaries. At the two side boundaries, the conditions of no viscous stress should be satisfied. Furthermore, there should be no flow across the side boundaries.

In this model, the key is the setting of the boundary condition at the oil/water interface. The impressed DC electric field exerts the electric force on interface charges, making the interface move. Furthermore, the movement of the interface is also affected by the shear stress from the nearby EOF. Owing to the viscous effect, the oil moves with the movement of the mobile interface and, meanwhile, applies shear stress to the interface to prevent the interface from moving. Therefore, at the oil/water interface, velocity continuum (eq 11a) and shear stress balance (eq 11b) should be met[12,36,37]

$$\boldsymbol{U}_w = \boldsymbol{U}_o \tag{11a}$$

$$\mu_w \frac{\partial \boldsymbol{U}_w}{\partial n} - \mu_o \frac{\partial \boldsymbol{U}_o}{\partial n} = \sigma_i \boldsymbol{E}_\perp \tag{11b}$$

In eq 11b, n denotes the normal direction to the oil/water interface; the term $\sigma_i \boldsymbol{E}_\perp$ is the electric stress acting on the interface, where $\boldsymbol{E}_\perp$ is the tangential component of the DC electric field at the interface, and σ_i stands for the interface charge density, given by[35]

$$\sigma_i = \frac{4zen_\infty}{\kappa} \sinh\left(\frac{ze\zeta_i}{2k_B T}\right) \tag{12}$$

where $\kappa = \sqrt{2n_\infty z^2 e^2/\varepsilon_0 \varepsilon k_B T}$ denotes the Debye–Hückel parameter.

It can be seen from eq 12 that the relative permittivity of the water (ε) greatly affects the charge density at the oil/water interface. The larger the parameter ε, the higher the charge density at the oil/water interface. However, the relative permittivity of the water is about 80 at room temperature. Thus, the parameter ε is set to 80, and the effect of the interfacial dielectric property on the interface charges is not considered in this work.

The EDL also forms near the particle/water interface, but compared with the particle size (10 μm in diameter), the EDL is thin and can be ignored. Therefore, to reduce the computation, this model does not consider the EDL formed near the particle surface. Instead, Helmholtz-Smoluchowski velocity (eq 13)[4,38] is adopted to reflect the EDL effect. Correspondingly, eq 6 is replaced by the zero-charge boundary condition.

$$\boldsymbol{U} = -\frac{\varepsilon_0 \varepsilon \zeta_s}{\mu} \boldsymbol{E} \tag{13}$$

where ζ_s is the zeta potential of the charged surface.

It should be noted that if the EDL produced at the oil/water interface also be ignored, the eq 11b will be invalid for the velocity gradient ($\frac{\partial \boldsymbol{U}_w}{\partial n}$) in the EDL becomes zero. Therefore, the EDL of the oil/water interface should be considered via adopting the PB equation (eqs 3 and 4) and the NS equation (eq 9).

For the particle/water interface, the boundary condition is as follows

$$\boldsymbol{U}_w = \boldsymbol{U}_p - \frac{\varepsilon_0 \varepsilon \zeta_p}{\mu_w} \boldsymbol{E} \tag{14}$$

where $\boldsymbol{U}_p$ stands for the particle translation velocity.

Since no EOF forms in the oil domain, the boundary condition of the particle/oil interface marked with blue color is

https://doi.org/10.1021/acsomega.1c05405
ACS Omega 2022, 7, 4062−4070

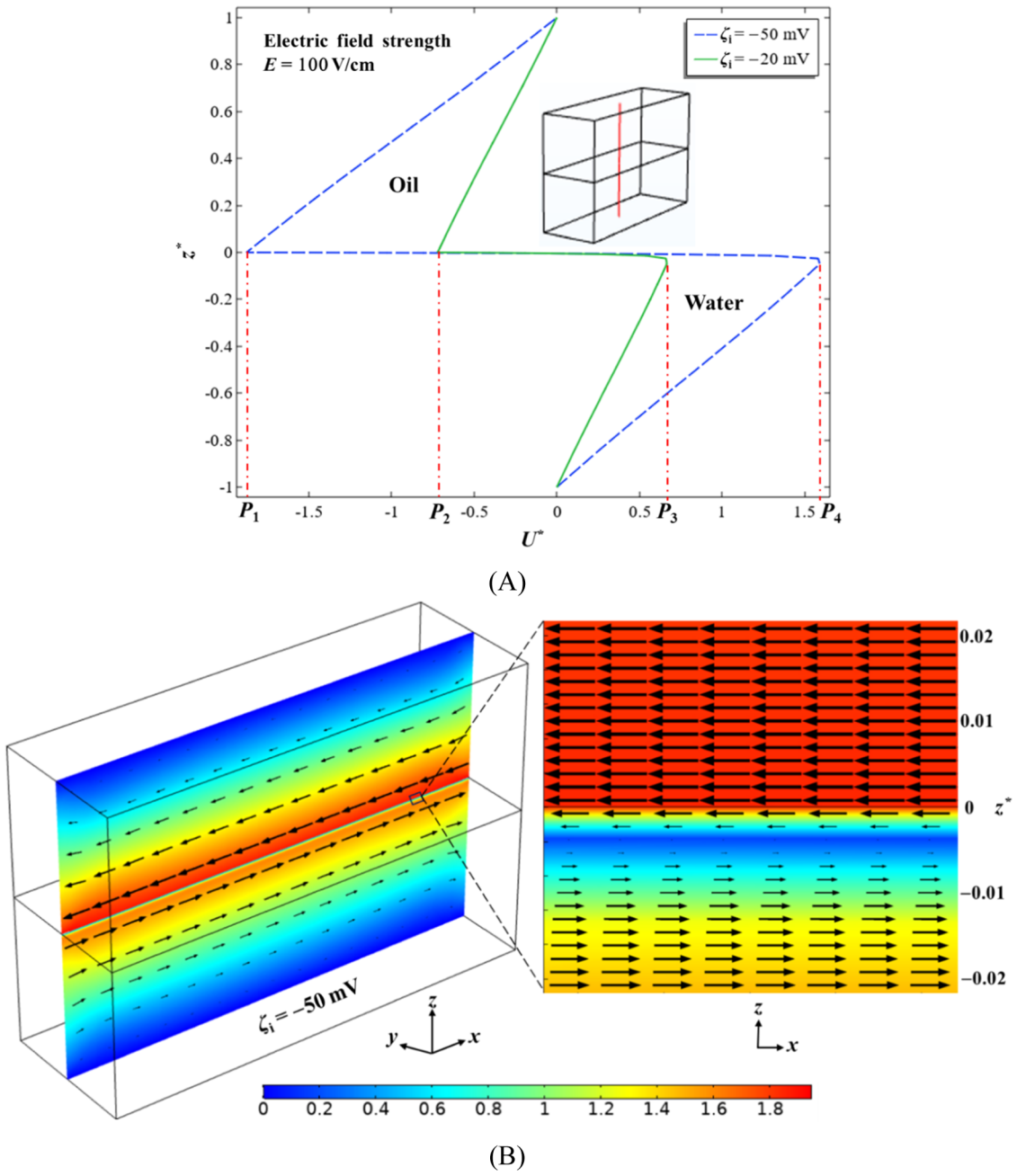

Figure 2. (A) Flow velocity profile along the z-coordinate (see the inset in this figure) and (B) flow field on the center plane in the steady state. P_1 and P_2 denote the moving velocity of the oil/water interface. P_1 to P_4 and P_2 to P_3 are the velocity profiles in the EDL formed at the interface. Arrows are the vector arrows of the flow field, and the color legend displays the magnitude of the dimensionless flow velocity ($z^* = z / H$; $U^* = U / U_{ref}$ and U_{ref} = 100 μm/s).

$$\boldsymbol{U}_o = \boldsymbol{U}_p \tag{15}$$

Once a DC electric field is applied to the water, the interface electrokinetic phenomenon drives the water and oil to flow. Thus, the particle will suffer a hydrodynamic force ($\boldsymbol{F}_o$) from the oil and a hydrodynamic force ($\boldsymbol{F}_w$) from the water. Meanwhile, the charged microparticle suffers an electric force. If the particle and the EDL formed around the particle surface are regarded as a whole object, the object is electrically neutral and only suffers a hydrodynamic force ($\boldsymbol{F}_w$) from the water. As the EDL formed near the particle surface is negligible in this model, the part of the microparticle submerged in water only experiences the hydrodynamic force ($\boldsymbol{F}_w$) mentioned above.[39,40] Therefore, the net force ($\boldsymbol{F}_p$) that makes the particle move is described as follows

$$\boldsymbol{F}_p = \boldsymbol{F}_o + \boldsymbol{F}_w \tag{16}$$

where the hydrodynamic forces of $\boldsymbol{F}_o$ and $\boldsymbol{F}_w$ are given by

$$\boldsymbol{F}_w = \int \{-P\boldsymbol{I} + \mu_w[\nabla \boldsymbol{U}_w + (\nabla \boldsymbol{U}_w)^T]\}\cdot \boldsymbol{n} dS_w \tag{17a}$$

$$\boldsymbol{F}_o = \int \{-P\boldsymbol{I} + \mu_o[\nabla \boldsymbol{U}_o + (\nabla \boldsymbol{U}_o)^T]\}\cdot \boldsymbol{n} dS_o \tag{17b}$$

where $\boldsymbol{I}$ and $\boldsymbol{n}$ are the second-order unit tensor and the unit normal vector of the boundary, respectively, and S_w and S_o

https://doi.org/10.1021/acsomega.1c05405
ACS Omega 2022, 7, 4062−4070

denote the particle surfaces in the water and the oil, respectively.

It is well-known that when the net force ($\boldsymbol{F}_p$) acting on the particle becomes zero, the particle velocity ($\boldsymbol{U}_p$) will become steady. As mentioned above, the microparticle at the interface suffers different hydrodynamic forces, resulting in a torque acting on the particle. However, because the oil/water interface has a strong surface tension, the particle is anchored at the interface, and the torque is counterbalanced. For example, under the conditions of the particle zeta potential $\zeta_p = -25$ mV, the interface zeta potential $\zeta_i = -50$ mV, the particle radius $R = 5$ μm, the electric field $E = 100$ V/cm, and the contact angle $\theta = 90°$, the two hydrodynamic forces the particle suffers are in the order of magnitude of 10^{-11} N. In contrast, for a typical interfacial tension of 50 mN/m,[41] the interfacial tension force the microparticle suffers is in the order of magnitude of 10^{-6} N. Thus, this model does not consider the rotational motion of the microparticle. In this work, the Joule heating effect is weak and can be ignored because of the low electric field strength (≤100 V/cm).[42] Additionally, since the polystyrene particle is very common and has a wide range of applications, this model takes the polystyrene microparticle as a typical particle. Considering that the polystyrene density is close to the water,[43] for simplicity, this model neglects the effect of the particle gravity. For the particle with a large density (e.g., metal particle), the effect of particle gravity on the interface should be considered.

3. NUMERICAL SIMULATION

A 3D simulation model is built in the software of COMSOL MULTIPHYSICS to solve the above theoretical model. Since mesh quality, especially the surface mesh quality of the oil/water interface and the surface of the microparticle, greatly affects the accuracy of the numerical result, the steady velocity of the particle was calculated by changing the mesh number. The calculation results indicate that when the mesh number is larger than 260,000, the particle velocity remains almost constant (see Figure S1 in Supporting Information). Hence, the mesh number is set to not less than 260,000 in the simulations.

As the study just focuses on the steady velocity of the microparticle absorbed at the interface, a simplified simulation method is proposed, as following: the particle is kept stationary, and the net force ($\boldsymbol{F}_p$) acting on the microparticle is calculated under different values of $\boldsymbol{U}_p$. Then, software can plot a figure about the evolution of $\boldsymbol{F}_p$ with $\boldsymbol{U}_p$. In this figure, the $\boldsymbol{U}_p$ that satisfies $\boldsymbol{F}_p = 0$ is the steady particle velocity. Compared with the traditional method using the time solver, the above method using the stationary solver can greatly reduce the computation and effectively save the calculation time. The model is also verified to evaluate the accuracy of the setting of the interface boundary conditions and the numerical method of the particle velocity used in this work. The details are shown in the Supporting Information.

In this work, the simulation is based on the method of finite element analysis. The non-equilibrium molecular dynamics simulation[44] may be a better method to investigate the more in-depth fundamental microscopic mechanism of the electrokinetic behavior of a single microparticle at a liquid−fluid interface.

4. RESULTS AND DISCUSSION

4.1. Flow Field in the Oil/Water Interface System. The steady flow field of the oil/water interface system under different interface zeta potentials (ζ_i) is displayed in Figure 2 (the DC electric field $\boldsymbol{E} = 100$ V/cm). As shown in Figure 2A, the negative value $\boldsymbol{U}^*$ ($\boldsymbol{U}^* = \boldsymbol{U} / \boldsymbol{U}_{ref}$, $\boldsymbol{U}_{ref} = 100$ μm/s) indicates that the liquid flows toward the positive electrode of the DC electric field, and the P_1 and P_2 are the moving velocities of the oil/water interface. P_1 to P_4 and P_2 to P_3 are the velocity profiles in the EDL formed at the interface.

It is clear that the negatively charged oil/water interface and the oil move toward the positive electrode of the electric field. The water outside the EDL, in contrast, flows toward the negative electrode. It could be understood as follows: it is well known that for the EOF generated near a solid surface, its velocity starts from zero at the surface and reaches the maximum at the EDL outer edge. However, different from a solid surface, the DC electric field could exert electric stress on the negatively charged oil/water interface, thereby dragging the mobile interface to move. Meanwhile, the EOF formed near the interface drives the water to flow to the negative electrode of $\boldsymbol{E}$ (see Figure 2B), hence, applies viscous stress to the interface. The moving oil/water interface drags the oil to flow with the interface via the viscous effect. Then, the flowing oil applies another viscous stress to the interface to prevent the interface from moving. The three stresses mentioned above are counterbalanced at the interface (eq 11b). Finally, the EOF is fully developed, and the flow field reaches steady. Compared with the two viscous stresses produced by the water and oil, the electric stress acting on the negative charge at the oil/water interface is greater, so the interface and the oil all move toward the positive electrode of $\boldsymbol{E}$. As the interface moving velocity is smaller than the EOF theoretical velocity (eq 13), the water outside the EDL still flows in the same direction as $\boldsymbol{E}$.

Based on eq 12, the larger the zeta potential value, the greater the interface charge density and, correspondingly, the higher the electric stress the interface suffers. Therefore, the oil/water interface moves faster under a higher interface zeta potential, as shown in Figure 2A; meanwhile, the water driven by the EOF generated near the interface also has a higher velocity (see eq 13). In addition, when the absolute values of ζ_i and $\boldsymbol{E}$ remain unchanged, the sign of ζ_i and the direction of $\boldsymbol{E}$ just affect the flow direction and do not affect the flow velocity (see Figure S4 of the Supporting Information and Figure 2).

When a negatively charged microparticle is adsorbed at the negatively charged interface, the particle will suffer an electric force (opposite direction as $\boldsymbol{E}$) from the electric field. Meanwhile, a hydrodynamic force (opposite direction as $\boldsymbol{E}$) from the oil and a hydrodynamic force (same direction as $\boldsymbol{E}$) from the water are also exerted on the particle (see "Abstract Graphic"), resulting in the motion of the particle at the interface. Therefore, the particle motion is greatly affected by the interface zeta potentials, the electric field, and the contact angle between the particle and the interface. In the following sections, the above key factors will be discussed in detail.

4.2. Effects of Interface Zeta Potentials on the Particle Velocity. Figure 3 shows the influence of the zeta potential of the oil/water interface (ζ_i) on the microparticle motion under the conditions of $\boldsymbol{E} = 100$ V/cm, $\zeta_p = -25$ mV, and $\theta = 90°$. Obviously, in an infinite oil/water interface system, the negatively charged microparticle at the negatively charged interface moves toward the positive electrode of $\boldsymbol{E}$,

https://doi.org/10.1021/acsomega.1c05405
ACS Omega 2022, 7, 4062−4070

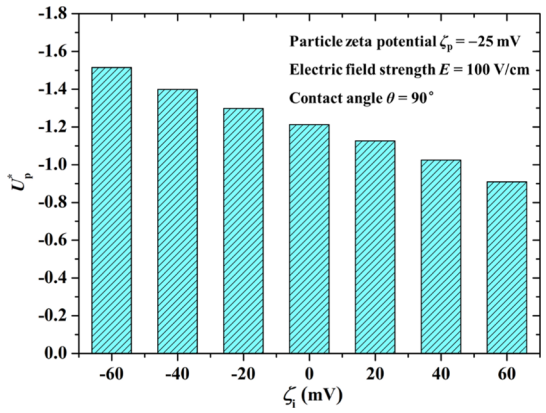

Figure 3. Dimensionless particle velocity as a function of the zeta potential of the oil/water interface. The negative value U_p^* ($U_p^* = U_p / U_{ref}$, U_{ref} = 100 μm/s) means the particle moves toward the positive electrode of the DC electric field, the same below.

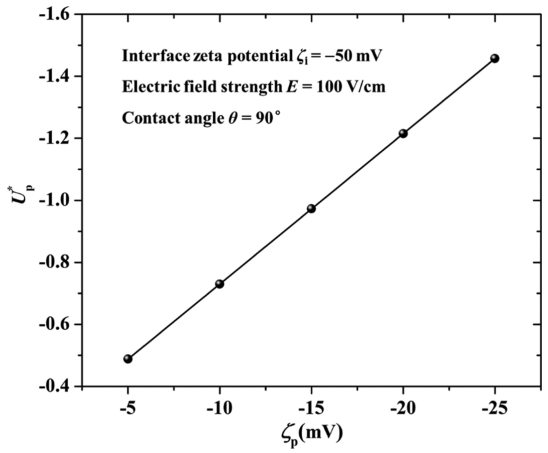

Figure 4. Dimensionless particle velocity as a function of the particle zeta potential.

and its velocity rises with the absolute value of ζ_i. When the oil/water interface is positively charged with a relatively small zeta potential, the negatively charged microparticle also moves toward the positive electrode of E, and its velocity decreases with ζ_i. The results could be understood as follows.

It can be observed in Figure 2 that the magnitude of the oil velocity is a little larger than that of the positive water velocity near the interface. Accordingly, the net hydrodynamic force, originated from the electrokinetic phenomenon generated at the interface, acting on the microparticle, is negative. Besides, under the effect of the DC electric field, the negatively charged microparticle is subjected to an electric force. Thus, the particle moves toward the positive electrode of the electric field. In Figure 2A, when the parameter ζ_i increases from −20 to −50 mV, the absolute value difference between the largest oil velocity and the largest water velocity rises from about 0.05 (the difference between absolute values of P_2 and P_3, as shown in Figure 2A) to about 0.26 (the difference between absolute values of P_1 and P_4, as shown in Figure 2A), engendering the increase in the abovementioned net hydrodynamic force. Thus, the particle moving velocity increases with the absolute value ζ_i. When ζ_i becomes positive, the net hydrodynamic force mentioned above also becomes positive and increases with ζ_i, resulting in the decline of the net force (opposite direction as E) acting on the particle. Accordingly, the particle moving velocity (opposite direction as E) decreases with the positive ζ_i, as shown in Figure 3.

If the DC electric field and the interface zeta potential remain constant, the flow field distribution and the corresponding net hydrodynamic force the microparticle suffers are fixed. Furthermore, the electric force the microparticle suffers increases linearly with the particle zeta potential (ζ_p), for the particle surface charge increases linearly with ζ_p.[35] Thus, one can easily understand that the particle velocity is proportional to the particle zeta potential (see Figure 4).

Comparing Figures 3 with 4, it can also be found that although the interface zeta potential has a great impact on the two-phase flow field (see Figure 2), its influence on the net hydrodynamic force is weak, as discussed above. Therefore, the effect of interface zeta potential on the particle velocity is weaker than that of the particle zeta potential.

Additionally, considering that one surface zeta potential will change with the concentration in reality,[45−47] and the effect of the concentration on the particle electrokinetic velocity is mainly reflected in its influence on the surface zeta potential, this work just focuses on the effect of the zeta potentials of the particle and the water/oil interface and does not carry out the study of the effect of the concentration under fixed surface zeta potentials.

4.3. Effect of DC Electric Field on the Particle Velocity. The dependence of the DC electric field (E) on the particle velocity under different contact angles between the particle and the interface is shown in Figure 5A. Clearly, the microparticle velocity linearly increases with E. First, with the increase in E, the velocities of both the water and the oil increase linearly because of the linear increase in the EOF velocity (see eq 13) and the electric stress (see eq 11b), resulting in the linear increase in the net hydrodynamic force exerting on the microparticle. Second, the electric force the particle suffers also linearly rises with E. Therefore, the results are easily understood in Figure 5A.

The particle material and the liquid are two key factors that determine the contact angle between the microparticle and the interface.[48,49] This work takes 60° (hydrophilic), 90°, and 120° (hydrophobic) as three typical examples. As this work considers that the oil/water interface remains horizontal, the relationship between the immersion depth (D) and the contact angle (θ) is $D = (1 + \cos\theta)R$. Thus, the corresponding immersion depths of the contact angle 60, 90, and 120° are 1.5R, R, and 0.5R, respectively.

As shown in Figure 5A, when the electric field remains constant, the particle velocity increases with the contact angle (θ). The reasons are as follows. The higher the contact angle (θ), the larger the contact area of the microparticle with oil and the corresponding force F_o (opposite direction as the electric field E) from the oil to the microparticle (see Figure 5B). The variation of the force (F_w) acting on the particle/water interface with θ is a little complicated. With the increase in θ, the contact area of the microparticle with water and the corresponding hydrodynamic force (positive direction as E) of the water to the microparticle will decline, while the electric force (negative direction as E) acting on the particle also decreases. From Figure 5B, it can be seen the direction of the force F_w is different under different contact angles, but the net force F_p remains in the opposite direction as E and increases with θ. Therefore, the microparticle moves faster with θ under the same electric field.

https://doi.org/10.1021/acsomega.1c05405
ACS Omega 2022, 7, 4062−4070

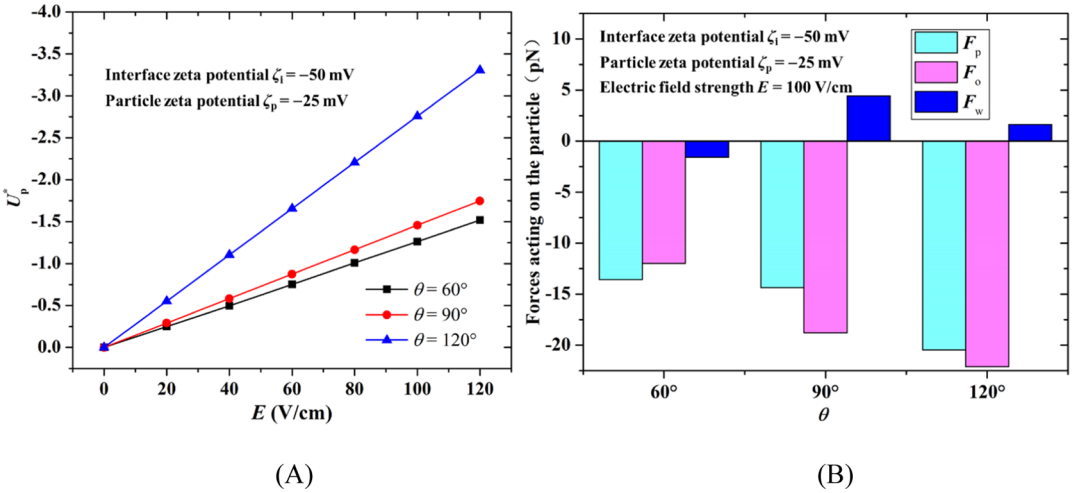

Figure 5. Dimensionless particle velocity as a function of electric field strength (A) and forces acting on the particle (B) under different contact angles.

4.4. Effect of Oil Dynamic Viscosity on the Particle Velocity. In the above sections, the dynamic viscosities of the water and the oil are set to be the same value ($\mu_w = \mu_o = 0.001$ Pa·s). If the dynamic viscosities are different, what will happen? Figure 6 displays the relationship between the oil dynamic viscosity and the microparticle moving velocity. It can be found that with the increase in the oil dynamic viscosity μ_o, the particle velocity declines and finally approaches zero. This phenomenon mentioned above could be explained as follows.

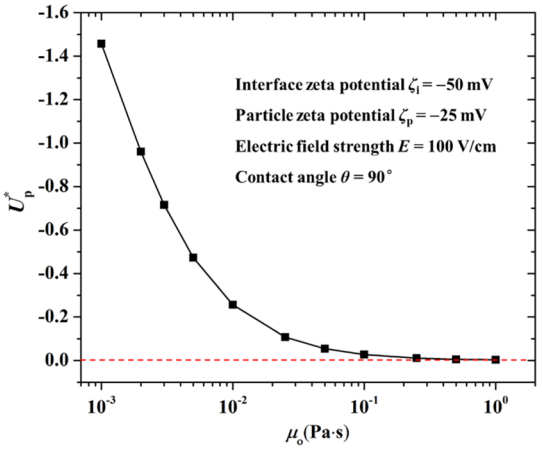

Figure 6. Dimensionless particle velocity as a function of oil dynamic viscosity.

When the dynamic viscosity of the oil (μ_o) is large enough, the flow resistance of the oil will become quite large; as a result, it is hard for the electrokinetic phenomenon generated at the interface to drive the interface and the corresponding oil. Accordingly, the microparticle seems to be fixed and almost cannot move at the interface. Therefore, it is not difficult to understand the result, as shown in Figure 6.

5. COMPARISON AND VERIFICATION

Zhang et al.[32] experimentally investigated the electrokinetic velocity of a polystyrene microparticle attached at a dodecane/water interface in a large container. The dynamic viscosity of dodecane used in their study is about 0.00136 Pa·s at room temperature. Their observations display that the contact angle between the polystyrene microparticle (10 μm in diameter) and the dodecane/water interface is about 140°. In their work, the reported zeta potentials of the polystyrene particle and the dodecane/water interface are −98 and −70 mV, respectively.

To verify the theoretical model established in this paper, the numerical simulation results obtained from this model are compared with Zhang's experiment results under the same conditions, as shown in Figure 7. The numerical study shows that the negatively charged particle moves toward the positive electrode of the electric field at a negatively charged interface, which matches Zhang's experiment results. Furthermore, the numerical simulation results for the electrokinetic velocity of a microparticle at the interface also agree with Zhang's experiment results. It should be pointed out that the electric field strength utilized in Zhang's experiment is weak (less than 10 V/cm). As the electric field strength increases, the Joule heating effect will become stronger, affecting the interface electrokinetic phenomenon and the particle velocity. Thus, when a strong electric field is applied, it is necessary to consider the Joule heating effect.

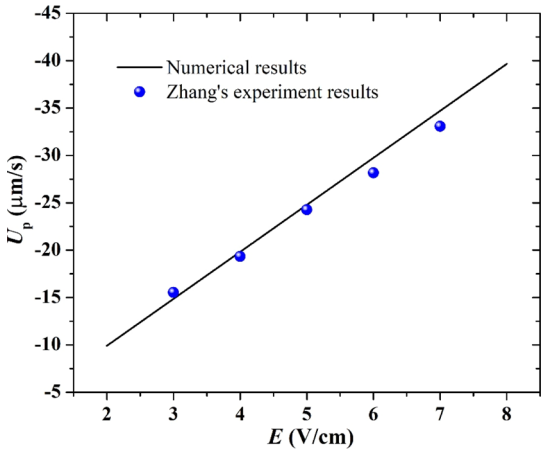

Figure 7. Comparison between the numerical results and Zhang's experiment results.[32] Reprinted from *Journal of Colloid and Interface Science*, 509, Zhang, J.; Song, Y.; Li, D, Electrokinetic Motion of a Spherical Polystyrene Particle at a Liquid−Fluid Interface, 432−439, Copyright (2018), with permission from Elsevier.

https://doi.org/10.1021/acsomega.1c05405
ACS Omega 2022, 7, 4062−4070

Additionally, this work considers that the microparticle is lowly charged with a relatively small zeta potential (−5 ∼ −25 mV), so the impact of the microparticle surface charge on the oil/water interface is ignored. In the case of a strong electric field, the interaction between a highly charged particle and the interface may become strong and should be considered. Overall, the model is verified qualitatively and can be further improved to satisfy different situations.

6. CONCLUSIONS

This work investigates the electrokinetic velocity of a charged microparticle at a horizontal oil/water interface in an infinite domain via a 3D simulation model. When a DC electric field is applied to the water along with the oil/water interface, the electrokinetic phenomenon formed at the charged interface drives the mobile interface to move, dragging the particle at the interface to move. The zeta potential, as well as the electric field, greatly affects the electrokinetic phenomena generated on a charged surface, and the contact angle between the particle and the interface determines the contact area of the microparticle with water and hence affects the microparticle motion. Thus, the impacts of these parameters on the particle velocity are emphatically studied and analyzed in this paper.

The results show that (1) for a negatively charged microparticle absorbed at a negatively charged oil/water interface in an infinite domain, the microparticle moves toward the positive electrode of the electric field, and its velocity increases along with the absolute values of zeta potential of both the particle and the oil/water interface, but the effect of interface zeta potential is quite weaker than that of the particle zeta potential; (2) if the oil/water interface is positively charged with a relatively small zeta potential, the negatively charged microparticle also moves toward the positive electrode of the electric field, which means that the direction of particle motion mainly depends on the sign of the particle zeta potential and the direction of the DC electric field; (3) the larger the contact angle, the faster the negatively charged microparticle moves at the negatively charged interface; and (4) the particle velocity declines with the rise of the oil dynamic viscosity. This study helps understand the electrokinetic behavior of microparticles at a liquid−fluid interface, which could be used in particle manipulation and material fabrication.

■ ASSOCIATED CONTENT

Supporting Information

The Supporting Information is available free of charge at https://pubs.acs.org/doi/10.1021/acsomega.1c05405.

Mesh independence test; model verification; and flow field under a positive oil/water interface zeta potential (PDF)

■ AUTHOR INFORMATION

Corresponding Author

Chengfa Wang − *Department of Marine Engineering, Dalian Maritime University, Dalian 116026, China;* orcid.org/0000-0002-5355-0490; Email: wangcf08@dlmu.edu.cn

Author

Qi Gao − *Department of Marine Engineering, Dalian Maritime University, Dalian 116026, China*

Complete contact information is available at: https://pubs.acs.org/10.1021/acsomega.1c05405

Notes

The authors declare no competing financial interest.

■ ACKNOWLEDGMENTS

This work is supported by the National Natural Science Foundation of China (52001050), the China Postdoctoral Science Foundation (2019M661083), the Natural Science Foundation of Liaoning Province (2021-BS-071), and the Fundamental Research Funds for the Central Universities (3132021208, 3132019192, 3132019336).

■ REFERENCES

(1) Cardenas-Benitez, B.; Jind, B.; Gallo-Villanueva, R. C.; Martinez-Chapa, S. O.; Lapizco-Encinas, B. H.; Perez-Gonzalez, V. H. Direct Current Electrokinetic Particle Trapping in Insulator-Based Microfluidics: Theory and Experiments. *Anal. Chem.* **2020**, *92*, 12871−12879.

(2) Xuan, X. Recent Advances in Direct Current Electrokinetic Manipulation of Particles for Microfluidic Applications. *Electrophoresis* **2019**, *40*, 2484−2513.

(3) Westermeier, R. *Electrophoresis in Practice: A Guide to Methods and Applications of DNA and Protein Separations*; Wiley-VCH: Weinheim, 2016; pp 7−51.

(4) Hunter, R. J. *Zeta Potential in Colloid Science: Principles and Applications*; Academic press: London, 1981; pp 1−58.

(5) Fang, H.; Wu, W.; Sang, Y.; Chen, S.; Zhu, X.; Zhang, L.; Niu, Y.; Gan, W. Evidence of the Adsorption of Hydroxide Ion at Hexadecane/Water Interface from Second Harmonic Generation Study. *RSC Adv.* **2015**, *5*, 23578−23585.

(6) Ma, A.; Xu, J.; Xu, H. Impact of Spontaneously Adsorbed Hydroxide Ions on Emulsification via Solvent Shifting. *J. Phys. Chem. C* **2014**, *118*, 23175−23180.

(7) Roger, K.; Cabane, B. Uncontaminated Hydrophobic/Water Interfaces Are Uncharged: A Reply. *Angew. Chem., Int. Ed.* **2012**, *124*, 13117−13119.

(8) Roger, K.; Cabane, B. Why Are Hydrophobic/Water Interfaces Negatively Charged? *Angew. Chem., Int. Ed.* **2012**, *51*, 5625−5628.

(9) Vácha, R.; Rick, S. W.; Jungwirth, P.; de Beer, A. G. F.; de Aguiar, H. B.; Samson, J.-S.; Roke, S. The Orientation and Charge of Water at the Hydrophobic Oil Droplet - Water Interface. *J. Am. Chem. Soc.* **2011**, *133*, 10204−10210.

(10) Creux, P.; Lachaise, J.; Graciaa, A.; Beattie, J. K.; Djerdjev, A. M. Strong Specific Hydroxide Ion Binding at the Pristine Oil/Water and Air/Water Interfaces. *J. Phys. Chem. B* **2009**, *113*, 14146−14150.

(11) Beattie, J. K.; Djerdjev, A. M. The Pristine Oil/Water Interface: Surfactant-Free Hydroxide-Charged Emulsions. *Angew. Chem., Int. Ed.* **2004**, *43*, 3568−3571.

(12) Gao, Y.; Wong, T. N.; Yang, C.; Ooi, K. T. Transient Two-Liquid Electroosmotic Flow with Electric Charges at the Interface. *Colloids Surf., A* **2005**, *266*, 117−128.

(13) Lee, J. S. H.; Li, D. Electroosmotic Flow at a Liquid-Air Interface. *Microfluid. Nanofluid.* **2006**, *2*, 361−365.

(14) Lee, J. S. H.; Barbulovic-Nad, I.; Wu, Z.; Xuan, X.; Li, D. Electrokinetic Flow in a Free Surface-Guided Microchannel. *J. Appl. Phys.* **2006**, *99*, 054905.

(15) Liu, W.; Ren, Y.; Tao, Y.; Chen, X.; Yao, B.; Hui, M.; Bai, L. Control of Two-Phase Flow in Microfluidics Using out-of-Phase Electroconvective Streaming. *Phys. Fluids* **2017**, *29*, 112002.

(16) Haiwang, L.; Wong, T. N.; Nguyen, N.-T. Time-Dependent Model of Mixed Electroosmotic/Pressure-Driven Three Immiscible Fluids in a Rectangular Microchannel. *Int. J. Heat Mass Transfer* **2010**, *53*, 772−785.

(17) Movahed, S.; Khani, S.; Wen, J. Z.; Li, D. Electroosmotic Flow in a Water Column Surrounded by an Immiscible Liquid. *J. Colloid Interface Sci.* **2012**, *372*, 207−211.

(18) Brask, A.; Goranović, G.; Bruus, H. Electroosmotic Pumping of Nonconducting Liquids by Viscous Drag from a Secondary Conducting Liquid. *Nanotech* **2003**, *1*, 190−193.
(19) Cooray, H.; Cicuta, P.; Vella, D. Floating and Sinking of a Pair of Spheres at a Liquid-Fluid Interface. *Langmuir* **2017**, *33*, 1427−1436.
(20) Dani, A.; Keiser, G.; Yeganeh, M.; Maldarelli, C. Hydrodynamics of Particles at an Oil−Water Interface. *Langmuir* **2015**, *31*, 13290−13302.
(21) Cohin, Y.; Fisson, M.; Jourde, K.; Fuller, G. G.; Sanson, N.; Talini, L.; Monteux, C. Tracking the Interfacial Dynamics of PNiPAM Soft Microgels Particles Adsorbed at the Air-Water Interface and in Thin Liquid Films. *Rheol. Acta* **2013**, *52*, 445−454.
(22) Cavallaro, M., Jr; Botto, L.; Lewandowski, E. P.; Wang, M.; Stebe, K. J. Curvature-Driven Capillary Migration and Assembly of Rod-like Particles. *Proc. Natl. Acad. Sci. U.S.A.* **2011**, *108*, 20923−20928.
(23) Dalbe, M.-J.; Cosic, D.; Berhanu, M.; Kudrolli, A. Aggregation of Frictional Particles Due to Capillary Attraction. *Phys. Rev. E: Stat., Nonlinear, Soft Matter Phys.* **2011**, *83*, 051403.
(24) Boneva, M. P.; Christov, N. C.; Danov, K. D.; Kralchevsky, P. A. Effect of Electric-Field-Induced Capillary Attraction on the Motion of Particles at an Oil-Water Interface. *Phys. Chem. Chem. Phys.* **2007**, *9*, 6371−6384.
(25) Singh, P.; Joseph, D. D. Fluid Dynamics of Floating Particles. *J. Fluid Mech.* **2005**, *530*, 31−80.
(26) Tarimala, S.; Ranabothu, S. R.; Vernetti, J. P.; Dai, L. L. Mobility and in Situ Aggregation of Charged Microparticles at Oil-Water Interfaces. *Langmuir* **2004**, *20*, 5171−5173.
(27) Nikolaides, M. G.; Bausch, A. R.; Hsu, M. F.; Dinsmore, A. D.; Brenner, M. P.; Gay, C.; Weitz, D. A. Electric-Field-Induced Capillary Attraction between like-Charged Particles at Liquid Interfaces. *Nature* **2002**, *420*, 299−301.
(28) Boneva, M. P.; Danov, K. D.; Christov, N. C.; Kralchevsky, P. A. Attraction between Particles at a Liquid Interface Due to the Interplay of Gravity- And Electric-Field-Induced Interfacial Deformations. *Langmuir* **2009**, *25*, 9129−9139.
(29) Li, M.; Li, D. Redistribution of Charged Aluminum Nanoparticles on Oil Droplets in Water in Response to Applied Electrical Field. *J. Nanopart. Res.* **2016**, *18*, 120.
(30) Li, M.; Li, D. Fabrication and Electrokinetic Motion of Electrically Anisotropic Janus Droplets in Microchannels. *Electrophoresis* **2017**, *38*, 287−295.
(31) Wang, C.; Li, M.; Song, Y.; Pan, X.; Li, D. Electrokinetic Motion of a Spherical Micro Particle at an Oil−water Interface in Microchannel. *Electrophoresis* **2018**, *39*, 807−815.
(32) Zhang, J.; Song, Y.; Li, D. Electrokinetic Motion of a Spherical Polystyrene Particle at a Liquid-Fluid Interface. *J. Colloid Interface Sci.* **2018**, *509*, 432−439.
(33) Masschaele, K.; Park, B. J.; Furst, E. M.; Fransaer, J.; Vermant, J. Finite Ion-Size Effects Dominate the Interaction between Charged Colloidal Particles at an Oil-Water Interface. *Phys. Rev. Lett.* **2010**, *105*, 048303.
(34) Uppapalli, S.; Zhao, H. The Influence of Particle Size and Residual Charge on Electrostatic Interactions between Charged Colloidal Particles at an Oil-Water Interface. *Soft Matter* **2014**, *10*, 4555−4560.
(35) Li, D. *Electrokinetics in Microfluidics*; Academic Press: London, 2004; pp 7−29.
(36) Wang, C.; Song, Y.; Pan, X.; Li, D. Translational Velocity of a Charged Oil Droplet Close to a Horizontal Solid Surface under an Applied Electric Field. *Int. J. Heat Mass Transfer* **2019**, *132*, 322−330.
(37) Wang, C.; Song, Y.; Pan, X.; Li, D. Electrokinetic Motion of a Submerged Oil Droplet near an Air−Water Interface. *Chem. Eng. Sci.* **2018**, *192*, 264−272.
(38) Probstein, R. F. *Physicochemical Hydrodynamics: An Introduction*; John Wiley & Sons: New York, 2005; pp 185−200.
(39) Wu, Z.; Li, D. Induced-Charge Electrophoretic Motion of Ideally Polarizable Particles. *Electrochim. Acta* **2009**, *54*, 3960−3967.
(40) Ai, Y.; Joo, S. W.; Jiang, Y.; Xuan, X.; Qian, S. Transient Electrophoretic Motion of a Charged Particle through a Converging-Diverging Microchannel: Effect of Direct Current-Dielectrophoretic Force. *Electrophoresis* **2009**, *30*, 2499−2506.
(41) Peng, Y.; Chen, W.; Fischer, T. M.; Weitz, D. A.; Tong, P. Short-Time Self-Diffusion of Nearly Hard Spheres at an Oil−Water Interface. *J. Fluid Mech.* **2009**, *618*, 243−261.
(42) Tang, G. Y.; Yang, C.; Chai, J. C.; Gong, H. Q. Joule Heating Effect on Electroosmotic Flow and Mass Species Transport in a Microcapillary. *Int. J. Heat Mass Transfer* **2004**, *47*, 215−227.
(43) Wu, J.; Dai, L. L. Apparent Microrheology of Oil−Water Interfaces by Single-Particle Tracking. *Langmuir* **2007**, *23*, 4324−4331.
(44) Kazemi, M.; Takbiri-Borujeni, A. Non-Equilibrium Molecular Dynamics Simulation of Gas Flow in Organic Nanochannels. *J. Nat. Gas Sci. Eng.* **2016**, *33*, 1087−1094.
(45) Gu, Y.; Li, D. The ζ-Potential of Silicone Oil Droplets Dispersed in Aqueous Solutions. *J. Colloid Interface Sci.* **1998**, *206*, 346−349.
(46) Yang, C.; Dabros, T.; Li, D.; Czarnecki, J.; Masliyah, J. H. Measurement of the Zeta Potential of Gas Bubbles in Aqueous Solutions by Microelectrophoresis Method. *J. Colloid Interface Sci.* **2001**, *243*, 128−135.
(47) Takahashi, M. ζ Potential of Microbubbles in Aqueous Solutions: Electrical Properties of the Gas−water Interface. *J. Phys. Chem. B* **2005**, *109*, 21858−21864.
(48) Chau, T. T.; Bruckard, W. J.; Koh, P. T. L.; Nguyen, A. V. A Review of Factors That Affect Contact Angle and Implications for Flotation Practice. *Adv. Colloid Interface Sci.* **2009**, *150*, 106−115.
(49) Paunov, V. N. Novel Method for Determining the Three-Phase Contact Angle of Colloid Particles Adsorbed at Air-Water and Oil-Water Interfaces. *Langmuir* **2003**, *19*, 7970−7976.

https://doi.org/10.1021/acsomega.1c05405
ACS Omega 2022, 7, 4062−4070